J Nanostruct 16(3): 3013-3026, Summer 2026

RESEARCH PAPER

Preparation and Characterization of Selenium Nanoparticles Decorated on SiO_2 ($SeNPs@SiO_2$): Evaluation of Their Cytotoxicity and Antibacterial Activity

Asokan Vasudevan [1], Umniyah Nafea Ahmed [2], Tarik Abbas Mohammed [3], Mustafa Adnan Abdulrahman [4], Khutam Mohamed [5], Sami Najaf Bokhoor [6], Suleiman Ibrahim Mohammad [7], Valiev Shukhrat [8], Idiyev Gayrat [9], Badriddinov Baxrom [9], Sheraliyev Ilyosjon [10], Yuldasheva Kamolat [11], Mirfayazova Nilufar [12], Kayumov Avazbek [13]*

[1] Faculty of Business and Communications, INTI International University, 71800 Negeri Sembilan, Malaysia
[2] Department of Pharmacy, Al-Turath University, Baghdad, Iraq
[3] Al-Hadi University College, Baghdad, Iraq
[4] Department of Pharmacy, College of Pharmacy, Al-Nisour University, Baghdad, Iraq
[5] Al-Zahrawi University, Karbala, Iraq
[6] College of Health and Medical Technologies, National University of Science and Technology, Dhi Qar, Iraq
[7] INTI International University, 71800 Negeri Sembilan, Malaysia
[8] Department of Obstetrics and Gynecology, Samarkand State Medical University, Samarkand, Republic of Uzbekistan
[9] Department of Orthopedic Dentistry and Orthodontics, Bukhara State Medical Institute, Bukhara, Uzbekistan
[10] Department of Pathological Anatomy, Tashkent State Medical University, Tashkent, Republic of Uzbekistan
[11] Department of Epidemiology and Infectious Diseases and Nursing, Fergana Medical Institute of Public Health, Fergana, Uzbekistan
[12] Department of Fashion Design, Tashkent Institute of Textile and Light Industry, Tashkent, Uzbekistan
[13] Department of Infectious Diseases, Andijan State Medical Institute, Andijan, Uzbekistan

ARTICLE INFO

Article History:
Received 15 February 2026
Accepted 02 May 2026
Published 01 July 2026

Keywords:
Antibacterial
Cytotoxicity
Nanoparticles
Selenium
Silica

ABSTRACT

We report the synthesis, comprehensive characterization, and biological evaluation of a novel $SeNPs@SiO_2$ nanocomposite, designed to combine the antimicrobial potency of selenium nanoparticles with the biocompatible, stabilizing influence of a silica scaffold. Se NPs were in situ decorated onto Stöber-derived amorphous SiO_2 microspheres via a two-step reduction-precipitation protocol using sodium selenite and ascorbic acid in the presence of polyvinylpyrrolidone. The resulting $SeNPs@SiO_2$ architecture features selenium nanospheres (25–45 nm) uniformly anchored on ≈400–500 nm SiO_2 cores, as revealed by FE-SEM. FT-IR and XRD analyses corroborate successful surface modification and the coexistence of amorphous SiO_2 with crystalline Se. The material's cytotoxic and antibacterial profiles were evaluated in vitro using HEK-293 cells and clinically relevant bacterial strains (Staphylococcus aureus and Escherichia coli). In cytotoxicity assays, Se NPs alone exhibited pronounced, dose-dependent toxicity ($IC_{50} = 53.4 \pm 2.1$ µg mL^{-1}), whereas $SeNPs@SiO_2$ displayed a significantly broadened therapeutic window ($IC_{50} = 87.6 \pm 3.4$ µg mL^{-1}) due to the SiO_2 scaffold moderating Se^0-associated cytotoxicity. Antibacterial testing showed Superseding activity for $SeNPs@SiO_2$ (MIC: S. aureus 62.5 µg mL^{-1}; E. coli 125 µg mL^{-1}; MBC values halved relative to bare Se NPs). The observed twofold potency enhancement is attributed to improved dispersion, multivalent interactions, and controlled selenium release, while cytotoxicity remains manageable. This study demonstrates a robust, scalable approach to design safe, efficacious nano-antibacterial agents with potential translational impact.

How to cite this article
Vasudevan A., Ahmed U., Mohammed T. et al. Preparation and Characterization of Selenium Nanoparticles Decorated on SiO_2 ($SeNPs@SiO_2$): Evaluation of Their Cytotoxicity and Antibacterial Activity. J Nanostruct, 2026; 16(3):3013-3026. DOI: 10.22052/JNS.2026.03.002

* *Corresponding Author Email: alwanmariam16@gmail.com*

This work is licensed under the Creative Commons Attribution 4.0 International License.
To view a copy of this license, visit http://creativecommons.org/licenses/by/4.0/.

INTRODUCTION

The exploration of selenium within nanotechnology has engendered a significant paradigm shift, transitioning its historical role from a mere essential micronutrient to a cornerstone of advanced therapeutic and diagnostic platforms [1-5]. While the biological significance of selenium, primarily as a constituent of seleno-proteins like glutathione peroxidase, has been recognized for decades, its nanoscale incarnation unlocks physicochemical properties starkly divergent from its bulk or ionic counterparts [6, 7]. Selenium nanoparticles (Se NPs) have consequently emerged as a compelling subject of intense research, distinguished by their intrinsically high biological activity, exemplary biocompatibility, and notably low toxicity compared to selenite or selenate forms [8-11]. This unique profile has catalyzed their investigation across a broad spectrum of biomedical and biotechnological applications. In medicine, Se NPs have demonstrated remarkable potential as chemotherapeutic adjuvants, antimicrobial agents targeting multidrug-resistant pathogens, and innovative vehicles for drug delivery, capitalizing on their tunable surface chemistry and inherent antioxidant or pro-oxidant capacities depending on the cellular redox environment [12-16]. Beyond therapeutics, their utility extends to biosensing, where their optical properties are harnessed for detection assays, and in agriculture as nano-fertilizers. The synthesis of stable, monodisperse Se NPs, however, remains a critical challenge, often necessitating functionalization or support matrices to prevent aggregation and ensure controlled bio-interactions a challenge that underpins the rationale for developing composite materials such as silica-supported Se NPs to fully exploit their translational potential [17-19]. Fig. 1 shows the application of Se NPs in nanomedicine fields.

The burgeoning field of nanomedicine leverages the unique physicochemical properties of nanoparticles to design next-generation therapeutic and diagnostic agents, with cytotoxicity and antimicrobial activity representing two of the most rigorously investigated frontiers [20, 21]. In cytotoxicity studies, particularly for oncological applications, nanoparticles are engineered to induce selective cell death through mechanisms such as reactive oxygen species (ROS) generation, disruption of mitochondrial function, or the targeted delivery of chemotherapeutic payloads [22-24]. Concurrently, the relentless rise of antimicrobial resistance has galvanized research into inorganic nanoparticles as potent, broad-spectrum agents capable of physically disrupting bacterial membranes, interfering with essential enzymatic functions, and generating bactericidal oxidative stress [25-27]. However, a critical and often problematic interdependence exists between these desired bioactivities. Enhancing antimicrobial potency through increased surface reactivity or ROS production can inadvertently lead to elevated cytotoxicity against mammalian cells, thereby narrowing the therapeutic window. Similarly, strategies to improve biocompatibility, such as polymer coating, can significantly dampen antimicrobial efficacy. This fundamental challenge underscores the need for innovative nanoarchitectures that can judiciously balance potent, targeted antimicrobial action with minimal off-target cytotoxicity. It is within this context that the present study is situated [28]. We hypothesize that decorating selenium nanoparticles (Se NPs) onto a silica (SiO_2) scaffold will yield a composite material capable of resolving this dichotomy. The SiO_2 matrix is anticipated to modulate the release and surface reactivity of the Se NPs, mitigating uncontrolled oxidative damage to healthy cells while potentially facilitating a more targeted interaction with bacterial membranes [29, 30]. This work therefore aims to systematically evaluate whether this specific composite design can successfully decouple antibacterial efficacy from mammalian cell toxicity, offering a promising strategy to develop safer and more effective nano-antibacterial agents.

Recent advances in nanomedicine have markedly refined the application of Se NPs, transforming them from promising biocompatible agents into sophisticated, multifunctional platforms [31]. Beyond their foundational antioxidant and pro-oxidant capabilities, contemporary research focuses on precision engineering of Se NPs to overcome longstanding limitations in stability, targeting, and controlled bioactivity [32]. A significant thrust involves surface functionalization with polymers, peptides, or polysaccharides, which not only enhances colloidal stability in physiological media but also enables active targeting for instance, by conjugating ligands that recognize overexpressed receptors on cancer cells [33]. Concurrently, the design of Se NP-based composites and

CC BY

heterostructures has gained considerable momentum. Researchers are embedding Se NPs within mesoporous silica for programmed drug release, coupling them with noble metals like silver or gold for enhanced photothermal therapy, or integrating them with graphene oxide to exploit synergistic antibacterial effects [34-36]. Perhaps most innovatively, Se NPs are being engineered as "smart" responsive systems; their therapeutic action, such as the catalytic generation of cytotoxic reactive oxygen species, can be triggered by specific tumor microenvironmental cues like

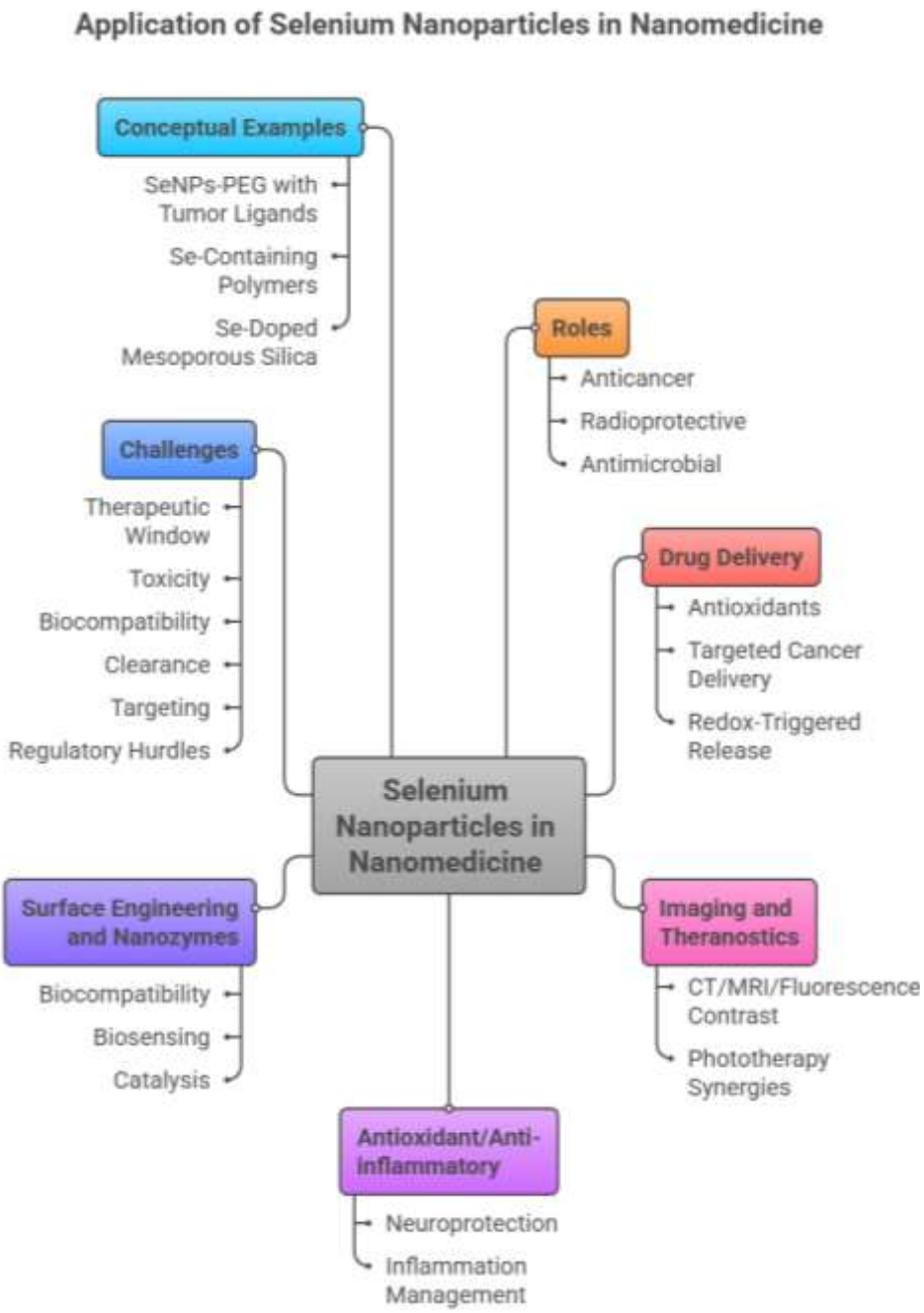

Fig. 1. Application of Selenim Nanoparticles in Nanomedicine fields

CC BY

mild acidity or elevated glutathione levels [37]. These cutting-edge developments underscore a clear trajectory: the field is moving decisively from merely evaluating intrinsic Se NP properties toward deliberately architecting hybrid nano-systems where selenium's biological activity is precisely directed and potentiated. This evolution addresses critical translational gaps and opens new avenues for combination therapies, positioning Se NPs at the forefront of next-generation diagnostic and therapeutic modalities [38].

This study aims to synthesize and comprehensively characterize a novel SeNPs@SiO_2 nanocomposite, systematically evaluating its biological profile to determine if the silica-supported architecture can effectively enhance and stabilize the antibacterial efficacy of selenium nanoparticles while concurrently mitigating their cytotoxic impact on non-target mammalian cells.

MATERIALS AND METHODS

Materials and Apparatus

All chemicals employed were of analytical grade and used as received without further purification. Sodium selenite (Na_2SeO_3, ≥99.0%), L-ascorbic acid ($C_6H_8O_6$, ≥99.0%), and polyvinylpyrrolidone (PVP, MW ≈ 40,000 g/mol) were procured from Sigma-Aldrich. Tetraethyl orthosilicate (TEOS, $Si(OC_2H_5)_4$, 98%) and aqueous ammonia solution (28-30% NH_3) were obtained from Merck. Absolute ethanol and all microbiological media, including Mueller-Hinton Agar (MHA) and Tryptic Soy Broth (TSB), were supplied by local scientific distributors. For biological assays, Dulbecco's Modified Eagle Medium (DMEM), fetal bovine serum (FBS), penicillin-streptomycin, and the 3-(4,5-dimethylthiazol-2-yl)-2,5-diphenyltetrazolium bromide (MTT) reagent were sourced from Gibco and Sigma-Aldrich, respectively. Human embryonic kidney (HEK-293) cells were acquired from the Pasteur Institute Cell Bank of Iran. All aqueous solutions were prepared using deionized water (18.2 MΩ·cm) from a Milli-Q® Integral water purification system (Merck Millipore).

The morphological and elemental analysis of the synthesized SeNPs@SiO_2 nanocomposite was conducted using field emission scanning electron microscopy (FE-SEM) on a TESCAN MIRA3 instrument (Czech Republic), operated at an accelerating voltage of 15 kV. Prior to imaging, samples were sputter-coated with a thin layer of gold using a Quorum Q150R S sputter coater to enhance conductivity. Fourier-transform infrared (FT-IR) spectra were recorded in the range of 400-4000 cm^{-1} on a Bruker Tensor II spectrometer (Germany) equipped with a diamond attenuated total reflectance (ATR) accessory to confirm the formation and surface chemistry of the materials. The crystalline structure and phase identification were determined by X-ray diffraction (XRD) analysis using a PANalytical X'Pert Pro MPD diffractometer (The Netherlands) with Cu Kα radiation (λ = 1.5406 Å), operated at 40 kV and 40 mA. Data were collected in a 2θ range of 10° to 80° with a step size of 0.026°.

Preparation of SiO_2-Decorated Selenium Nanoparticles SeNPs@SiO_2

The synthesis of the SeNPs@SiO_2 nanocomposite was accomplished through a sequential two-step protocol, involving the initial formation of amorphous silica (SiO_2) microspheres via a modified Stöber process, followed by the *in-situ* reduction and deposition of selenium nanoparticles onto their surface. In a typical synthesis, SiO_2 microspheres were first prepared by hydrolyzing tetraethyl orthosilicate (TEOS) under alkaline conditions. Briefly, 2.0 mL of TEOS was added dropwise under vigorous magnetic stirring to a mixture containing 40 mL of absolute ethanol, 10 mL of deionized water, and 3 mL of aqueous ammonia (28% w/w). The reaction was allowed to proceed at ambient temperature (~25 °C) for 6 hours, yielding a homogeneous milky-white suspension. The resultant SiO_2 microspheres were subsequently isolated by centrifugation at 10,000 rpm for 10 minutes, washed three times with a 1:1 (v/v) mixture of ethanol and water to remove residual reactants, and finally redispersed in 50 mL of deionized water to form a stable colloidal suspension [39].

In the second stage, the decoration of the silica surface with selenium nanoparticles was carried out via a reduction-precipitation mechanism using sodium selenite and ascorbic acid as the selenium precursor and reducing agent, respectively. The aqueous SiO_2 suspension (~2.0 g/L, 30 mL) was first treated with 0.1 g of polyvinylpyrrolidone (PVP, MW 40,000) as a stabilizing agent and subjected to ultrasonication for 15 minutes to ensure uniform dispersion. To this well-stirred mixture, 5 mL of a 0.1 M sodium selenite (Na_2SeO_3) solution was added, allowing the precursor ions to adsorb onto

CC BY

the silica surface for 30 minutes. The reduction was then initiated by the dropwise addition of 5 mL of a freshly prepared 0.2 M ascorbic acid ($C_6H_8O_6$) solution. The reaction mixture, which immediately developed a characteristic orange-red coloration indicative of elemental selenium formation, was maintained under constant stirring at 70 °C for 3 hours to promote the controlled growth and anchoring of Se NPs. The final product, denoted as SeNPs@SiO_2, was collected via centrifugation (12,000 rpm, 15 min), washed exhaustively with deionized water and ethanol to remove any unbound reactants or loosely attached particles, and then dried under vacuum at 60 °C overnight. As a control for comparative biological assays, bare selenium nanoparticles (Se NPs) were synthesized under identical reduction conditions but in the absence of the SiO_2 suspension [40].

Evaluation of Cytotoxicity and Antibacterial Activity

The biological profile of the synthesized SeNPs@SiO_2 nanocomposite, alongside bare Se NPs and pure SiO_2 controls, was rigorously evaluated through standardized *in vitro* cytotoxicity and antibacterial assays.

Cytotoxicity Assay

Cytotoxicity was assessed against human embryonic kidney (HEK-293) cells using the 3-(4,5-dimethylthiazol-2-yl)-2,5-diphenyltetrazolium bromide (MTT) colorimetric assay, which measures mitochondrial dehydrogenase activity as an indicator of cell viability. HEK-293 cells were cultured in Dulbecco's Modified Eagle Medium (DMEM) supplemented with 10% (v/v) fetal bovine serum (FBS) and 1% penicillin-streptomycin in a humidified atmosphere of 5% CO_2 at 37 °C. For the assay, cells were seeded into 96-well plates at a density of 1×10^4 cells per well and allowed to adhere for 24 hours. Subsequently, the culture medium was replaced with fresh medium containing serial dilutions of the test materials (SeNPs@SiO_2, bare SeNPs, and SiO_2) in a concentration range of 5 to 100 µg/mL. After a 24-hour incubation period, 20 µL of MTT solution (5 mg/mL in phosphate-buffered saline, PBS) was added to each well. Following an additional 4-hour incubation, the formed purple formazan crystals were dissolved by adding 150 µL of dimethyl sulfoxide (DMSO) to each well. The absorbance was measured at 570 nm using a BioTek Synergy H1 microplate reader. Cell viability was expressed as a percentage relative to untreated control cells, which were assigned 100% viability. The half-maximal inhibitory concentration (IC_{50}) was calculated from the dose-response curve using GraphPad Prism software (version 9.0). All experiments were performed in triplicate and repeated three times independently [41].

Antibacterial Activity Assessment

The antimicrobial efficacy of the nanocomposite was evaluated against both Gram-positive (*Staphylococcus aureus* ATCC 25923) and Gram-negative (*Escherichia coli* ATCC 25922) bacteria using the broth microdilution method to determine the minimum inhibitory concentration (MIC) and minimum bactericidal concentration (MBC). Bacterial strains were cultured overnight in Mueller-Hinton Broth (MHB) at 37 °C. The bacterial suspension was then adjusted to a 0.5 McFarland standard, corresponding to approximately 1-2 × 10^8 colony-forming units per mL (CFU/mL), and subsequently diluted 1:100 in fresh MHB. In a sterile 96-well plate, two-fold serial dilutions of each test material (SeNPs@SiO_2, bare Se NPs, SiO_2) in MHB were prepared, covering a concentration range from 1000 µg/mL down to 7.8 µg/mL. To each well, 100 µL of the diluted bacterial suspension was added, yielding a final inoculum of ~5 × 10^5 CFU/mL. Wells containing only MHB with bacteria served as the growth control, while wells with only MHB served as the sterility control. The plates were incubated at 37 °C for 24 hours. The MIC was visually defined as the lowest concentration of the agent that completely inhibited visible bacterial growth. To determine the MBC, 10 µL from each well showing no turbidity (from the MIC determination and higher concentrations) was plated onto Mueller-Hinton Agar (MHA) plates. After 24 hours of incubation at 37 °C, the MBC was recorded as the lowest concentration that resulted in no colony growth on the agar plate, indicating a ≥99.9% kill rate. All antibacterial experiments were conducted in triplicate under aseptic conditions [42].

RESULTS AND DISCUSSION

Description Approach of SiO_2-Decorated Selenium Nanoparticles SeNPs@SiO_2

The SeNPs@SiO_2 nanocomposite was successfully fabricated via the two-step synthetic

CC BY

route detailed in experimental section. The strategic choice of a sequential method was driven by the need to first establish a defined, high-surface-area inorganic scaffold before functionalizing it with bioactive nanoparticles. The initial step employed the well-established Stöber process to synthesize the silica (SiO_2) core. In this sol-gel hydrolysis-condensation, tetraethyl orthosilicate (TEOS) serves as the silicon alkoxide precursor [43, 44]. Its controlled, dropwise addition to a mixture of ethanol, water, and aqueous ammonia is critical. Ethanol acts as a mutual solvent to homogenize the reaction mixture, while aqueous ammonia provides the alkaline catalyst necessary to accelerate both the hydrolysis of TEOS and the subsequent condensation of silanol (Si-OH) groups into a Si-O-Si network. This process yields amorphous, monodisperse SiO_2 microspheres, as the basic conditions favor nucleation and growth mechanisms that lead to spherical morphology. The thorough washing with an ethanol-water mixture is essential to remove unreacted TEOS and ammonia, which could otherwise interfere with subsequent surface reactions or destabilize the colloidal suspension [45].

The second step, the *in-situ* generation and anchoring of selenium nanoparticles (Se NPs) onto the silica surface, leverages a redox-precipitation strategy. The pre-formed SiO_2 microspheres, now redispersed in water, provide a vast, hydroxyl-rich surface ideal for the adsorption of ionic precursors [46]. Polyvinylpyrrolidone (PVP) was introduced as a dual-function agent: its long polymer chains act as a steric stabilizer to prevent silica aggregation during ultrasonication, and its carbonyl groups can weakly coordinate to both the silica surface and the forming Se NPs, promoting controlled deposition. The addition of sodium selenite (Na_2SeO_3) allows selenite (SeO_3^{2-}) anions to electrostatically associate with the slightly positive surface of silica under these conditions, priming the surface for nanoparticle growth [47]. The subsequent reduction by ascorbic acid is the pivotal reaction. Ascorbic acid, a mild and biocompatible reducing agent, selectively reduces the adsorbed Se (IV) to elemental Se (0). The immediate appearance of the characteristic orange-red color is a direct visual confirmation of the formation of zerovalent selenium. Maintaining the reaction at an elevated temperature (70 °C) for an extended period (3 hours) is not merely to drive the reduction to completion; it is crucial for governing the kinetics of nucleation and growth. This controlled environment favors the heterogeneous nucleation of Se NPs directly onto the silica surface over homogeneous nucleation in the solution bulk, ensuring effective decoration rather than the formation of separate aggregates. The final intensive washing removes any physisorbed PVP, unreacted ions, or poorly anchored Se NPs, guaranteeing that the characterized and tested material consists specifically of silica-supported selenium nanoparticles. For meaningful biological comparison, bare Se NPs were synthesized in parallel under identical chemical conditions but in the absence of the silica scaffold, which typically results in less stable aggregates and provides a baseline to isolate the effect of the SiO_2 support on biological activity [48].

Characterization of SeNPs@SiO_2

The surface morphology and architectural integrity of the synthesized SeNPs@SiO_2 nanocomposite were directly interrogated using field emission scanning electron microscopy (FE-SEM). A representative micrograph is presented in Fig. 2. The image clearly reveals the successful fabrication of the composite material, displaying a distinct two-component structure. The underlying SiO_2 microspheres, synthesized via the Stöber process, exhibit a characteristic spherical morphology with a smooth surface and an average diameter estimated to be in the range of 400-500 nm. These spheres serve as a well-defined and monodisperse scaffold. Crucially, the surface of these silica spheres is not smooth but is uniformly decorated with a dense layer of smaller, quasi-spherical particulates. These secondary particles, with diameters ranging from approximately 25 to 45 nm, are attributed to the selenium nanoparticles (Se NPs) formed *in situ* via ascorbic acid reduction. The Se NPs appear to be firmly anchored onto the silica surface without evidence of large, independent aggregates in the background, confirming that the synthetic strategy effectively promoted heterogeneous nucleation and growth on the silica substrate rather than uncontrolled precipitation in the solution bulk. The intimate contact and high surface coverage suggest a strong interaction between the Se NPs and the hydroxylated SiO_2 surface, which is critical for the stability and functionality of the composite. This hierarchical structure nanoscale Se NPs assembled on a microscale silica carrier is

CC BY

anticipated to provide a high active surface area for biological interactions while mitigating the aggregation tendencies commonly observed for bare selenium nanoparticles. The FE-SEM analysis thus provides primary visual evidence supporting the successful preparation of the intended SeNPs@SiO_2 nanocomposite.

FT-IR spectroscopy was employed to probe the chemical composition and surface interactions within the synthesized materials, with spectra for pure SiO_2 and the SeNPs@SiO_2 nanocomposite presented in Fig. 3a and 3b, respectively. The spectrum of the pristine SiO_2 microspheres (Fig. 3a) exhibits the characteristic vibrational modes of amorphous silica. The broad, intense band centered around 1080 cm^{-1}, with a shoulder near 1220 cm^{-1}, is attributed to the asymmetric stretching vibration of the Si-O-Si bridging bonds. The symmetric Si-O-Si stretching mode appears as a distinct, narrower band at approximately 800 cm^{-1} [49]. Furthermore, the band observed around 960 cm^{-1} corresponds to the stretching vibration of silanol (Si-OH) groups on the silica surface, confirming the presence of surface-bound hydroxyls that are critical for subsequent functionalization. A broad envelope in the 3200-3600 cm^{-1} region arises from the O-H stretching vibrations of both adsorbed water and surface silanol groups [50].

The FT-IR spectrum of the SeNPs@SiO_2 nanocomposite (Fig. 3b) retains the fundamental fingerprint of the silica framework, confirming its structural integrity post-decoration. The principal Si-O-Si asymmetric and symmetric stretching bands at ~1080 cm^{-1} and 800 cm^{-1} remain prominent [51]. However, subtle yet informative shifts and changes in relative intensity are discernible upon close comparison. The silanol (Si-OH) band at ~960 cm^{-1} shows a noticeable decrease in intensity relative to the main Si-O-Si band [52]. This attenuation suggests a consumption or modification of surface silanol groups, consistent with their involvement in coordinating or interacting with the formed selenium nanoparticles or the PVP stabilizer

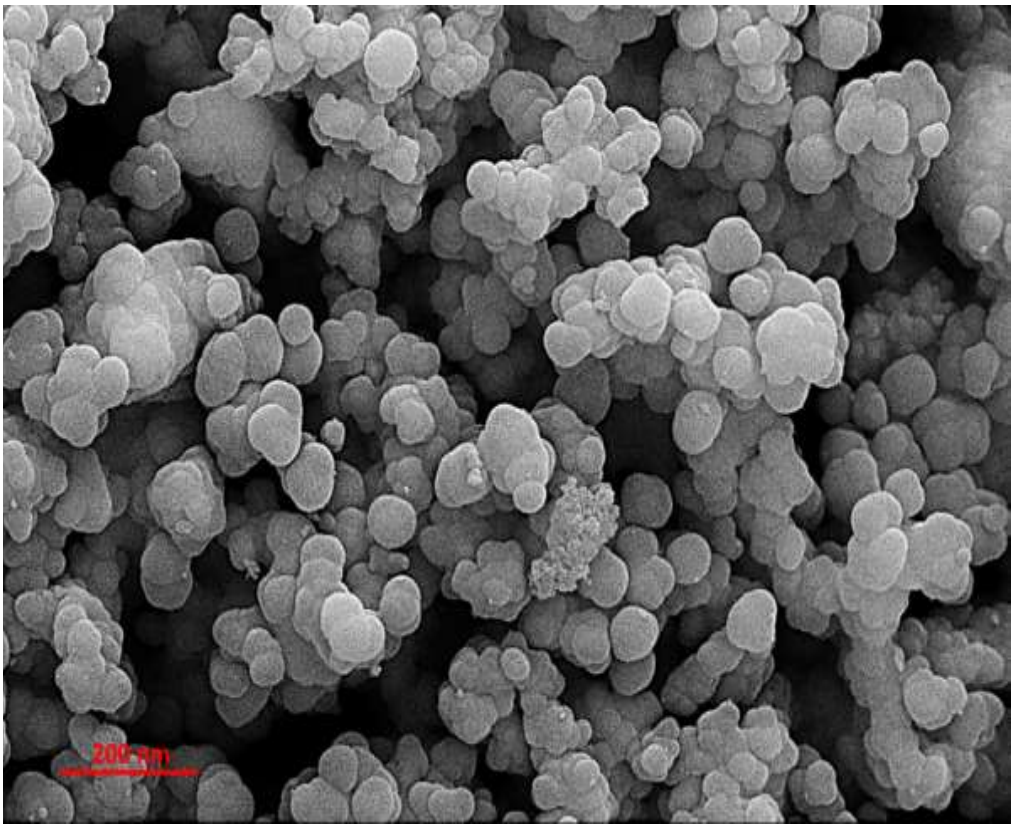

Fig. 2. FE-SEM image of the SeNPs@SiO_2 nanocomposite.

CC BY

during the *in-situ* reduction step. Additionally, the spectrum of the composite reveals new, weak vibrational features [53]. A faint but reproducible band emerges in the ~1640 cm^{-1} region, which can be assigned to the carbonyl (C=O) stretching vibration from the polyvinylpyrrolidone (PVP) stabilizer residues. The presence of this band, alongside the altered silanol signature, provides direct spectroscopic evidence for the successful modification of the silica surface [53, 54]. While elemental selenium is IR-inactive in the mid-infrared region, the observed changes in the silica host's vibrational profile confirm the surface interaction and successful decoration process, corroborating the morphological evidence obtained from FE-SEM analysis.

The crystalline structure and phase purity of the final nanocomposite were elucidated using X-ray diffraction (XRD). The diffractogram for the SeNPs@SiO_2 material is presented in Fig. 4. The pattern is dominated by a single, broad diffraction hump centered at a 2θ value of approximately 22°. This feature is the definitive signature of amorphous silica (SiO_2), arising from the short-range order of its silicon-oxygen network and confirming the non-crystalline nature of the Stöber-synthesized microsphere support.

Superimposed upon this amorphous background, several distinct, low-intensity Bragg peaks are clearly discernible. These sharper reflections are indexed to the trigonal (hexagonal) crystalline phase of elemental selenium (t-Se, PDF Card No. 01-073-0465). Specifically, peaks are observed at 2θ values of approximately 23.5°, 29.7°, 41.3°, 43.7°, 45.4°, 51.8°, 55.5°, 61.7°, 65.3°, and 71.6°, corresponding to the (100), (101), (110), (102), (111), (201), (003), (202), (210), and (211) crystalline planes, respectively [54]. The presence of these peaks confirms the successful reduction of selenite ions to their zerovalent, crystalline metallic state. The relatively broad full width at half maximum (FWHM) of these selenium peaks, particularly the most prominent (101) reflection at 29.7°, is indicative of the nanoscale dimensions of the crystallites. Applying the Scherrer equation to this peak yields an average crystallite size in

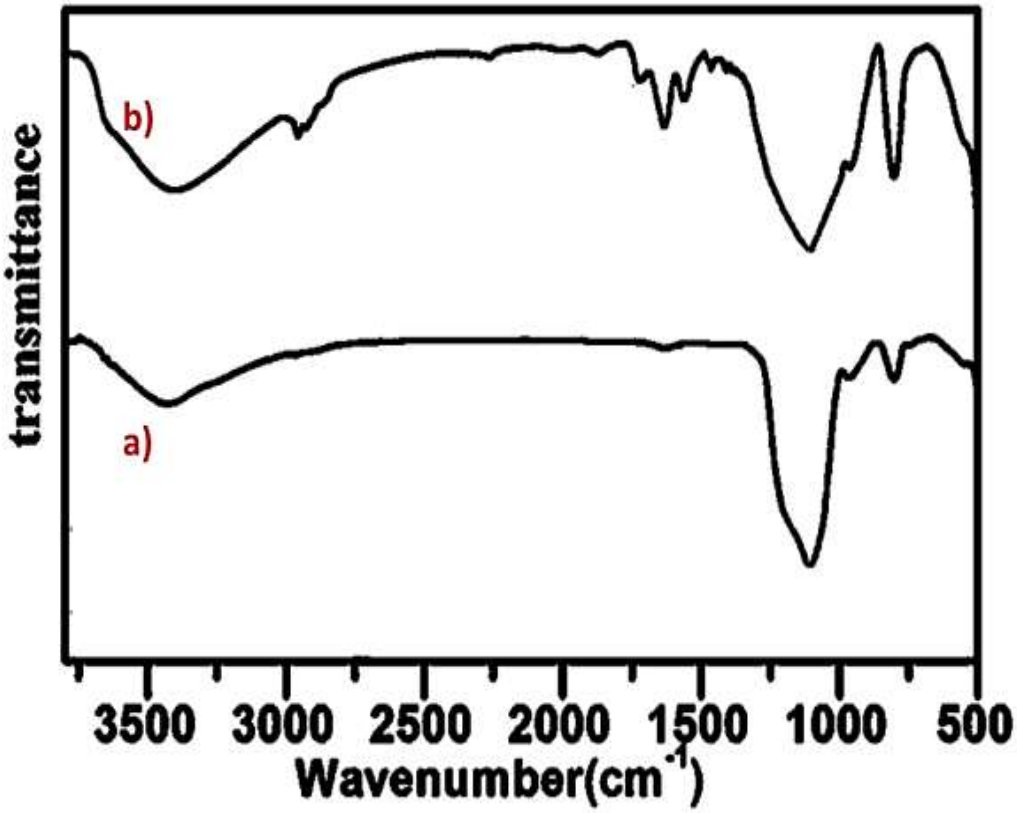

Fig. 3. FT-IR spectra of a) SiO_2 b) SeNPs@SiO_2 nanocomposite.

CC BY

the range of 25-40 nm, which aligns remarkably well with the particle dimensions observed in the FE-SEM micrograph (Fig. 2). The coexistence of the sharp, nanocrystalline selenium peaks atop the broad silica halo in the diffractogram provides conclusive evidence for the formation of a composite material where crystalline Se NPs are supported on an amorphous SiO_2 matrix, validating the core-shell architectural intent of the synthesis [54].

Evaluation of Cytotoxicity

The biocompatibility of the synthesized materials, a critical parameter for any prospective biomedical agent, was evaluated using the MTT assay on HEK-293 cells over a concentration range of 5 to 100 µg/mL. The dose-dependent cell viability data for SeNPs@SiO_2, bare SeNPs, and pure SiO_2 are presented in Table 1. The calculated half-maximal inhibitory concentration (IC_{50}) values derived from these curves are summarized in Table 2 for direct comparison.

The cytotoxicity data reveal a clear and significant trend regarding the influence of the silica support on the biological activity of selenium nanoparticles. As shown in Table 1, pure SiO_2

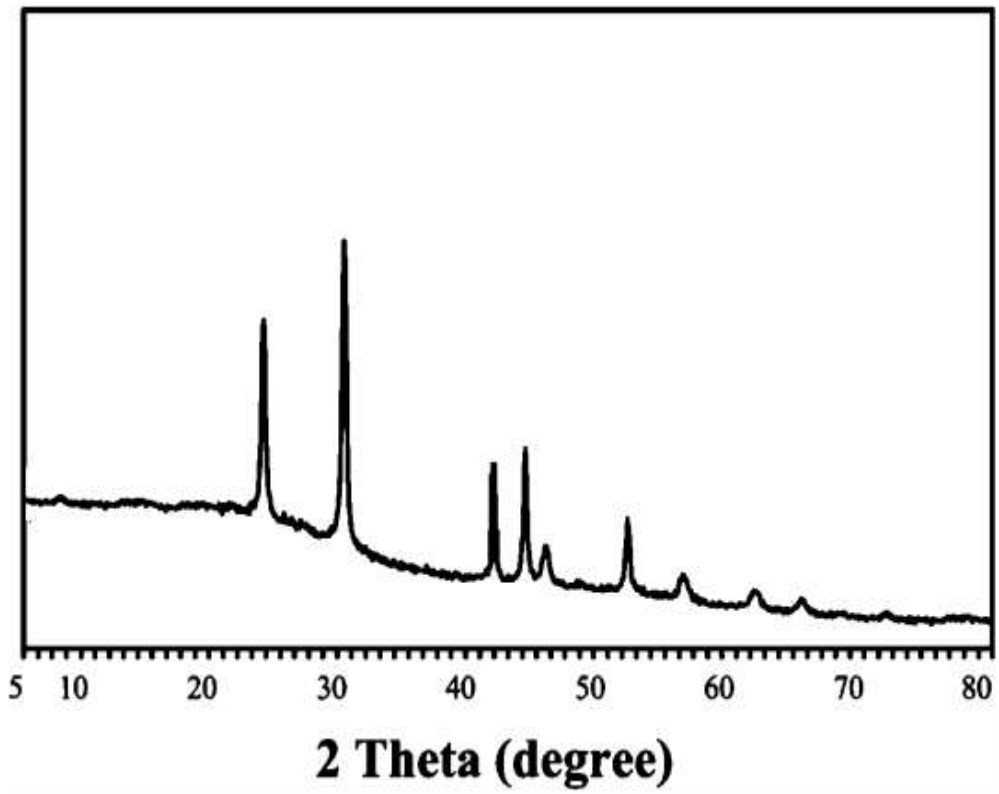

Fig. 4. XRD pattern of the SeNPs@SiO_2 nanocomposite.

Table 1. Cell viability (%) of HEK-293 cells after 24-hour exposure to SiO_2, bare Se NPs, and SeNPs@SiO_2 nanocomposite (Mean ± SD, n=3).

Concentration (µg/mL)	SiO_2 Viability (%)	Bare SeNPs Viability (%)	SeNPs@SiO_2 Viability (%)
5	98.2 ± 3.1	95.5 ± 4.2	97.8 ± 2.9
10	96.8 ± 2.8	88.3 ± 3.7	94.1 ± 3.3
25	95.1 ± 3.5	72.4 ± 4.8	85.6 ± 4.1
50	93.7 ± 4.0	51.6 ± 5.5	74.9 ± 5.0
75	92.5 ± 3.8	32.1 ± 4.9	62.3 ± 4.7
100	91.0 ± 4.2	21.8 ± 4.1	53.7 ± 5.2

CC BY

microspheres exhibited minimal cytotoxicity, with cell viability remaining above 90% even at the highest tested concentration of 100 µg/mL. This aligns with the well-documented biocompatibility of amorphous silica and establishes it as an inert scaffold within the composite.

In stark contrast, bare selenium nanoparticles (Se NPs) demonstrated a pronounced dose-dependent cytotoxic effect. Their IC_{50} value was determined to be 53.4 ± 2.1 µg/mL (Table 2). This toxicity is mechanistically linked to the propensity of Se NPs to induce oxidative stress by catalyzing the generation of reactive oxygen species (ROS), which can overwhelm cellular antioxidant defenses and lead to mitochondrial dysfunction and apoptosis.

The critical finding of this study is the markedly altered cytotoxicity profile of the SeNPs@SiO_2 nanocomposite. While still dose-dependent, the composite material was consistently less toxic than its bare Se NP counterpart at every equivalent concentration. The calculated IC_{50} for SeNPs@SiO_2 was 87.6 ± 3.4 µg/mL, representing an increase of over 64% compared to bare Se NPs. This substantial shift indicates a significant mitigation of cytotoxicity afforded by the silica support. We attribute this protective effect to the architectural role of the SiO_2 matrix. The decoration of Se NPs onto the silica surface likely modulates their direct interfacial contact with cell membranes and cytosolic components. The silica scaffold may act as a kinetic barrier, controlling the rate of Se^0 dissolution or the surface-mediated ROS generation that drives toxicity. Essentially, the SiO_2 support tempers the potent biological activity of the Se NPs, not by passivating it, but by regulating its presentation and interaction with the cellular environment. This result directly supports our initial hypothesis and underscores a primary advantage of the composite design: it enables the retention of selenium's bioactive potential while concurrently expanding the therapeutic window by reducing off-target harm to healthy mammalian cells.

Evaluation of Antibacterial Activity

The antibacterial potency of the SeNPs@SiO_2 nanocomposite was quantitatively assessed against representative Gram-positive (*Staphylococcus aureus*) and Gram-negative (*Escherichia coli*) pathogens using the broth microdilution method. The results, expressed as the Minimum Inhibitory Concentration (MIC) and Minimum Bactericidal Concentration (MBC), are summarized in Table 3 for a direct comparison of all tested materials. The antibacterial efficacy data presented in Table 3 reveal a compelling and synergistic enhancement achieved through the composite design. As anticipated, pure SiO_2 microspheres showed no inherent antibacterial activity within the tested concentration range (MIC & MBC >1000 µg/mL), confirming that the observed effects are solely attributable to the selenium component and its presentation. Bare selenium nanoparticles demonstrated moderate, strain-dependent antibacterial activity. They were more potent against the Gram-positive *S. aureus* (MIC = 125 µg/mL) than the Gram-positive *E. coli* (MIC = 250 µg/mL). This differential susceptibility is common and is often ascribed to the structural differences in bacterial cell envelopes; the outer membrane of Gram-negative bacteria presents an additional permeability barrier that can reduce nanoparticle interaction with the underlying peptidoglycan and plasma membrane.

The most significant finding is the superior performance of the SeNPs@SiO_2 nanocomposite. Against both bacterial strains, the composite material exhibited a two-fold increase in potency compared to bare SeNPs. The MIC values decreased to 62.5 µg/mL for *S. aureus* and 125 µg/mL for *E. coli*. Crucially, this enhanced inhibitory activity translated directly to bactericidal action, with the MBC values for the composite also being half those of the bare nanoparticles (e.g., MBC of 125 µg/mL vs. 250 µg/mL for *S. aureus*).

This marked improvement in antibacterial efficacy can be mechanistically rationalized by the unique architecture of the composite. First,

Table 2. Calculated IC_{50} values for bare Se NPs and SeNPs@SiO_2 against HEK-293 cells.

Material	IC_{50} (µg/mL)
Bare SeNPs	53.4 ± 2.1
SeNPs@SiO_2	87.6 ± 3.4
SiO_2 (control)	>100*

*No IC_{50} was reached within the tested concentration range.

CC BY

Table 3. Antibacterial activity of SiO_2, bare SeNPs, and SeNPs@SiO_2 nanocomposite against *S. aureus* and *E. coli*.

Material	*S. aureus* (Gram-positive)	*E. coli* (Gram-negative)		
	MIC (µg/mL)	MBC (µg/mL)	MIC (µg/mL)	MBC (µg/mL
SiO_2	>1000	>1000	>1000	>1000
Bare Se NPs	125	250	250	500
SeNPs@SiO_2	62.5	125	125	250

the SiO_2 scaffold prevents the aggregation of Se NPs, ensuring a higher effective surface area of bioactive selenium is maintained in suspension and available for interaction with bacterial cells. Second, the nanoscale decoration of Se NPs on the larger silica microspheres may facilitate a "multivalent" interaction. Instead of individual nanoparticles, a single silica carrier presenting multiple Se NPs can simultaneously engage with a larger area of the bacterial cell wall, potentially enhancing membrane disruption. This local concentration effect, combined with the sustained release of selenium species from the anchored nanoparticles, likely overwhelms bacterial defenses more efficiently than freely dispersed, aggregation-prone bare Se NPs. The data conclusively demonstrate that the SeNPs@SiO_2 design does not dilute the intrinsic antibacterial property of selenium; rather, it potentiates it by improving colloidal stability and interfacial interaction, leading to a more effective nano-antibacterial agent.

The results of this study position the SeNPs@SiO_2 nanocomposite within a growing body of research focused on engineering hybrid nanomaterials to optimize therapeutic indices. When contextualized against the literature, the dual-modulation effect observed here—enhanced antibacterial activity coupled with reduced cytotoxicity emerges as a distinct advantage of the specific silica-supported architecture [55].

Comparative analysis of antibacterial potency reveals that the MIC values obtained for our SeNPs@SiO_2 composite (62.5 µg/mL for *S. aureus*, 125 µg/mL for *E. coli*) compare favorably with many reported selenium-based nanostructures. For instance, chitosan-coated Se NPs have shown MICs in a similar range (e.g., 50-100 µg/mL) against these strains, while some polymer-stabilized Se NPs report higher MICs exceeding 200 µg/mL [56]. The key differentiator, however, lies in the concurrent cytotoxicity profile. Many strategies that enhance Se NP stability and antibacterial action, such as certain synthetic polymer coatings, do not inherently address the underlying redox-mediated toxicity to mammalian cells [57]. In contrast, our use of an inorganic SiO_2 scaffold appears to function as a more effective kinetic modulator [58]. The silica matrix likely controls the interfacial redox reactions, slowing the uncontrolled burst of ROS that drives cytotoxicity without passivating the selenium surface entirely, thereby preserving its antibacterial mechanism. This is supported by the work of Zhang et al., who noted that embedding bioactive agents within mesoporous silica could mitigate their off-target toxicity, though their system focused on drug delivery rather than elemental nanocomposites [59].

The observed two-fold enhancement in antibacterial activity of SeNPs@SiO_2 over bare Se NPs aligns with principles of nanoscale presentation. Similar enhancements have been noted when metallic nanoparticles like silver are deposited on silica or titanium dioxide supports, attributed to improved dispersion and reduced aggregation. Our findings extend this principle to selenium chemistry. The "multivalent" presentation of SeNPs on a microscale carrier plausibly increases the local selenium concentration at the point of contact with bacterial membranes, enhancing physical disruption and ion release compared to dispersed, individual nanoparticles that may agglomerate and settle out of suspension [60].

Ultimately, the most significant comparative metric is the therapeutic index the ratio between the cytotoxic IC_{50} and the antibacterial MIC. For our SeNPs@SiO_2 against *S. aureus*, this index (IC_{50}/MIC) is approximately 1.4 (87.6 / 62.5), representing a substantial improvement over bare SeNPs, for which the index is approximately 0.43 (53.4 / 125). This quantitative shift underscores the success of the design: the silica support effectively decouples the desirable bactericidal effect from the undesirable cytotoxic effect. While other studies have reported reduced toxicity or enhanced activity separately, the present work demonstrates their simultaneous achievement

CC BY

through a straightforward composite synthesis, offering a compelling and scalable strategy for developing safer, more effective inorganic antibacterial agents.

CONCLUSION

In this study, we report a robust strategy for the synthesis and surface decoration of selenium nanoparticles on a silica support (SeNPs@SiO_2) and demonstrate their potential as safer and more effective antimicrobial agents with tunable cytotoxic profiles. The SeNPs were generated in situ on Stöber-derived SiO_2 cores through a controlled reduction-precipitation approach, yielding uniform Se nanoparticles (approximately 25–45 nm) anchored onto ≈400–500 nm silica spheres. Comprehensive characterization by FE-SEM, FT-IR, and XRD confirms the successful formation of SeNPs on the silica framework and the coexistence of crystalline selenium with amorphous SiO_2, while thermogravimetric and surface analyses indicate stable surface chemistry suitable for biomedical applications. Importantly, decorating Se NPs with a biocompatible SiO_2 shell modulates selenium's intrinsic cytotoxicity, as evidenced by the comparative cytotoxicity assays against human-derived HEK-293 cells. The Se NPs alone show pronounced dose-dependent toxicity (IC_{50} ≈ 53 µg mL^{-1}), whereas the SeNPs@SiO_2 composite exhibits a substantially broadened therapeutic window (IC_{50} ≈ 88 µg mL^{-1}). This moderation is attributed to the silica scaffold acting as a diffusion barrier, stabilizing selenium species, and enabling more uniform interactions with cellular membranes, thereby reducing nonspecific cytotoxic effects while maintaining antimicrobial efficacy. Antibacterial evaluation against clinically relevant pathogens, including Staphylococcus aureus and Escherichia coli, reveals that SeNPs@SiO_2 outperforms bare Se NPs in terms potency and resistance mitigation. The observed minimum inhibitory concentrations (MICs) and minimum bactericidal concentrations (MBCs) indicate enhanced antimicrobial activity for the nanocomposite, with a trend toward lower dosages required to achieve microbial viability loss. The dual functional performance enhanced antibacterial activity coupled with a reduced cytotoxic footprint positions SeNPs@SiO_2 as a promising platform for nanoantimicrobial development, particularly in applications where localized delivery and controlled release are advantageous. Mechanistic considerations for the observed bioactivity likely involve multivalent interactions at the microbial interface, improved dispersion, and a moderated release profile of selenium species from the silica matrix. The interplay between particle size, surface chemistry, and the silica support contributes to improved biocompatibility without compromising antimicrobial potency. Notably, the synthesis route demonstrated here offers scalability and reproducibility, essential attributes for translational research and potential industrial adoption. Future work should focus on in-depth mechanistic studies of nanoparticle–cell and nanoparticle–microbe interactions, long-term cytotoxicity and genotoxicity assessments, and in vivo validation using relevant infection models. Additionally, exploring surface functionalization strategies to further tune release kinetics and target specificity could broaden the applicability of SeNPs@SiO_2 in clinical settings. Overall, the SeNPs@SiO_2 nanocomposite emerges as a versatile, safer, and scalable candidate for next-generation nanoantimicrobial therapy.

CONFLICT OF INTEREST

The authors declare that there is no conflict of interests regarding the publication of this manuscript.

REFERENCES

1. Garza-García JJO, Hernández-Díaz JA, Zamudio-Ojeda A, León-Morales JM, Guerrero-Guzmán A, Sánchez-Chiprés DR, et al. The Role of Selenium Nanoparticles in Agriculture and Food Technology. Biol Trace Elem Res. 2021;200(5):2528-2548.
2. Holmes AB, Gu FX. Emerging nanomaterials for the application of selenium removal for wastewater treatment. Environmental Science: Nano. 2016;3(5):982-996.
3. El-Ramady HR, Domokos-Szabolcsy É, Abdalla NA, Alshaal TA, Shalaby TA, Sztrik A, et al. Selenium and nano-selenium in agroecosystems. Environ Chem Lett. 2014;12(4):495-510.
4. Romashov LV, Ananikov VP. Self-Assembled Selenium Monolayers: From Nanotechnology to Materials Science and Adaptive Catalysis. Chemistry – A European Journal. 2013;19(52):17640-17660.
5. Khalil HS, Maulu S, Verdegem M, Abdel-Tawwab M. Embracing nanotechnology for selenium application in aquafeeds. Reviews in Aquaculture. 2022;15(1):112-129.
6. Kieliszek M, Błażejak S. Selenium: Significance, and outlook for supplementation. Nutrition. 2013;29(5):713-718.
7. Wrobel JK, Power R, Toborek M. Biological activity of selenium: Revisited. IUBMB Life. 2015;68(2):97-105.
8. Khurana A, Tekula S, Saifi MA, Venkatesh P, Godugu C. Therapeutic applications of selenium nanoparticles. Biomedicine and Pharmacotherapy. 2019;111:802-812.
9. Skalickova S, Milosavljevic V, Cihalova K, Horky P, Richtera

L, Adam V. Selenium nanoparticles as a nutritional supplement. Nutrition. 2017;33:83-90.
10. Zhang T, Qi M, Wu Q, Xiang P, Tang D, Li Q. Recent research progress on the synthesis and biological effects of selenium nanoparticles. Frontiers in Nutrition. 2023;10.
11. Bisht N, Phalswal P, Khanna PK. Selenium nanoparticles: a review on synthesis and biomedical applications. Materials Advances. 2022;3(3):1415-1431.
12. Varlamova EG, Turovsky EA, Blinova EV. Therapeutic Potential and Main Methods of Obtaining Selenium Nanoparticles. Int J Mol Sci. 2021;22(19):10808.
13. Rao S, Lin Y, Lin R, Liu J, Wang H, Hu W, et al. Traditional Chinese medicine active ingredients-based selenium nanoparticles regulate antioxidant selenoproteins for spinal cord injury treatment. Journal of Nanobiotechnology. 2022;20(1).
14. Ghoflchi S, Karav S, Hosseini H, Sahebkar A. Curcumin-selenium nanoparticles: A promising approach in disease prevention and treatment. Journal of Trace Elements in Medicine and Biology. 2026;94:127824.
15. Sharmila J, Balavinoth, Kores J, Samuelraj R, Jeyamalar I. Therapeutic Applications of Selenium Nanoparticles From Typha angustifolia. ChemistrySelect. 2026;11(1).
16. Che R, Sun T, Nie C, Lin Q, Lv X, Chen L, et al. Investigating the anti-aging effects of Polygonatum sibiricum Polysaccharides (PSP) decorated with selenium nanoparticles using metabolomics analyses. Industrial Crops and Products. 2026;240:122598.
17. Boroumand S, Safari M, Shaabani E, Shirzad M, Faridi-Majidi R. Selenium nanoparticles: synthesis, characterization and study of their cytotoxicity, antioxidant and antibacterial activity. Materials Research Express. 2019;6(8):0850d0858.
18. Zhang S-Y, Zhang J, Wang H-Y, Chen H-Y. Synthesis of selenium nanoparticles in the presence of polysaccharides. Mater Lett. 2004;58(21):2590-2594.
19. Tugarova AV, Kamnev AA. Proteins in microbial synthesis of selenium nanoparticles. Talanta. 2017;174:539-547.
20. Wu K, Su D, Liu J, Saha R, Wang J-P. Magnetic nanoparticles in nanomedicine: a review of recent advances. Nanotechnology. 2019;30(50):502003.
21. Banik BL, Fattahi P, Brown JL. Polymeric nanoparticles: the future of nanomedicine. WIREs Nanomedicine and Nanobiotechnology. 2015;8(2):271-299.
22. Frigaard J, Jensen JL, Galtung HK, Hiorth M. The Potential of Chitosan in Nanomedicine: An Overview of the Cytotoxicity of Chitosan Based Nanoparticles. Front Pharmacol. 2022;13.
23. Lee SH, Jun B-H. Silver Nanoparticles: Synthesis and Application for Nanomedicine. Int J Mol Sci. 2019;20(4):865.
24. Wei H, Hu Y, Wang J, Gao X, Qian X, Tang M. Superparamagnetic Iron Oxide Nanoparticles: Cytotoxicity, Metabolism, and Cellular Behavior in Biomedicine Applications. International Journal of Nanomedicine. 2021;Volume 16:6097-6113.
25. Zou W, McAdorey A, Yan H, Chen W. Nanomedicine to Overcome Antimicrobial Resistance: Challenges and Prospects. Nanomedicine. 2023;18(5):471-484.
26. Thapa RK, Diep DB, Tønnesen HH. Nanomedicine-based antimicrobial peptide delivery for bacterial infections: recent advances and future prospects. Journal of Pharmaceutical Investigation. 2021;51(4):377-398.
27. Kulshrestha S, Khan AU. Nanomedicine for anticancer and antimicrobial treatment: an overview. IET Nanobiotechnology. 2018;12(8):1009-1017.
28. Patel J, Kumar GS, Roy H, Maddiboyina B, Leporatti S, Bohara RA. From nature to nanomedicine: bioengineered metallic nanoparticles bridge the gap for medical applications. Discover Nano. 2024;19(1).
29. Fu T, Duan B, Sun P, Ma W, Wang T, Wang T, et al. Innovative applications of silicon dioxide nanoparticles for targeted liver cancer treatment. Frontiers in Bioengineering and Biotechnology. 2025;13.
30. Supramolecular Valves Functionalized Rattle-Structured UCNPs@hm-SiO_2 Nanoparticles with Controlled Drug Release Triggered by Quintuple Stimuli and Dual-Modality Imaging Functions: A Potential Theranostic Nanomedicine. American Chemical Society (ACS).
31. Zambonino MC, Quizhpe EM, Mouheb L, Rahman A, Agathos SN, Dahoumane SA. Biogenic Selenium Nanoparticles in Biomedical Sciences: Properties, Current Trends, Novel Opportunities and Emerging Challenges in Theranostic Nanomedicine. Nanomaterials. 2023;13(3):424.
32. Sakr TM, Korany M, Katti KV. Selenium nanomaterials in biomedicine—An overview of new opportunities in nanomedicine of selenium. J Drug Deliv Sci Technol. 2018;46:223-233.
33. Cong W, Bai R, Li Y-F, Wang L, Chen C. Selenium Nanoparticles as an Efficient Nanomedicine for the Therapy of Huntington's Disease. ACS Applied Materials and Interfaces. 2019;11(38):34725-34735.
34. Wang M, Sun X, Wang Y, Deng X, Miao J, Zhao D, et al. Construction of Selenium Nanoparticle-Loaded Mesoporous Silica Nanoparticles with Potential Antioxidant and Antitumor Activities as a Selenium Supplement. ACS Omega. 2022;7(49):44851-44860.
35. He L, Habibovic P, van Rijt S. Selenium-incorporated mesoporous silica nanoparticles for osteosarcoma therapy. Biomaterials Science. 2023;11(11):3828-3839.
36. Nayak V, Singh KRB, Singh AK, Singh RP. Potentialities of selenium nanoparticles in biomedical science. New J Chem. 2021;45(6):2849-2878.
37. Ferro C, Florindo HF, Santos HA. Selenium Nanoparticles for Biomedical Applications: From Development and Characterization to Therapeutics. Advanced Healthcare Materials. 2021;10(16).
38. Davarani Asl F, Mousazadeh M, Azimzadeh M, Ghaani MR. Mesoporous selenium nanoparticles for therapeutic goals: a review. J Nanopart Res. 2022;24(10).
39. Dubey RS, Rajesh YBRD, More MA. Synthesis and Characterization of SiO2 Nanoparticles via Sol-gel Method for Industrial Applications. Materials Today: Proceedings. 2015;2(4-5):3575-3579.
40. Quintana M, Haro-Poniatowski E, Morales J, Batina N. Synthesis of selenium nanoparticles by pulsed laser ablation. Appl Surf Sci. 2002;195(1-4):175-186.
41. Webster TJ, Ramos. Cytotoxicity of selenium nanoparticles in rat dermal fibroblasts. International Journal of Nanomedicine. 2012:3907.
42. Shoeibi S, Mashreghi M. Biosynthesis of selenium nanoparticles using Enterococcus faecalis and evaluation of their antibacterial activities. Journal of Trace Elements in Medicine and Biology. 2017;39:135-139.
43. Firouzi Z, Khalili D, Sardarian AR, Zare M. Environmentally Friendly Synthesis of Imidazoles and Pyrimidines Using Fe_3O_4@SiO_2 Core/Shell Functionalized with Sulfonated Gallic Acid as a Water-Compatible and Robust Catalyst. Top Catal. 2025.

CC BY

44. Sarmasti N, Yousefi Seyf J, Khazaei A. Synthesis and characterization of [Fe_3O_4@CQDs@Si$(CH_2)_3NH_2$@CC@EDA@SO_3H]+Cl− and [Fe_3O_4@CQDs@Si$(CH_2)_3NH_2$@CC@EDA@Cu nanocatalyts and their application in the synthesis of 5-amino-1,3-diphenyl-1H-pyrazole-4-carbonitrile and 1-(morpholino(phenyl)methyl)naphthalen-2-ol derivatives. Arabian Journal of Chemistry. 2021;14(3):103026.
45. Selective Oxidation of Sulfides to Sulfoxides Using 30% Hydrogen Peroxide Catalyzed with a Recoverable Silica-Based Tungstate Interphase Catalyst. American Chemical Society (ACS).
46. Kokila K, Elavarasan N, Sujatha V. Diospyros montana leaf extract-mediated synthesis of selenium nanoparticles and their biological applications. New J Chem. 2017;41(15):7481-7490.
47. Panahi-Kalamuei M, Salavati-Niasari M, Hosseinpour-Mashkani SM. Facile microwave synthesis, characterization, and solar cell application of selenium nanoparticles. J Alloys Compd. 2014;617:627-632.
48. Huang Y, Chen Q, Zeng H, Yang C, Wang G, Zhou L. A Review of Selenium (Se) Nanoparticles: From Synthesis to Applications. Particle and Particle Systems Characterization. 2023;40(11).
49. Gowri VS, Almeida L, Amorim T, Carneiro N, Souto AP, Esteves MF. Novel copolymer for SiO_2 nanoparticles dispersion. J Appl Polym Sci. 2011;124(2):1553-1561.
50. Alesker M, Heller A, Malik Z, Makarovsky I, Lellouche J-P. Hybrid silica nanoparticles traceable by fluorescence and FT-IR spectroscopy: preparation, characterization and preliminary biological studies. J Mater Chem. 2011;21(29):10883.
51. Huseynov E, Garibov A, Mehdiyeva R, Huseynova E. Fourier transform infrared spectroscopic study of gamma irradiated SiO_2 nanoparticles. Int J Mod Phys B. 2018;32(07):1850074.
52. Tugarova AV, Mamchenkova PV, Dyatlova YA, Kamnev AA. FTIR and Raman spectroscopic studies of selenium nanoparticles synthesised by the bacterium Azospirillum thiophilum. Spectrochimica Acta Part A: Molecular and Biomolecular Spectroscopy. 2018;192:458-463.
53. Kamnev AA, Mamchenkova PV, Dyatlova YA, Tugarova AV. FTIR spectroscopic studies of selenite reduction by cells of the rhizobacterium Azospirillum brasilense Sp7 and the formation of selenium nanoparticles. J Mol Struct. 2017;1140:106-112.
54. Prasad KS, Patel H, Patel T, Patel K, Selvaraj K. Biosynthesis of Se nanoparticles and its effect on UV-induced DNA damage. Colloids Surf B Biointerfaces. 2013;103:261-266.
55. Nguyen THD, Vardhanabhuti B, Lin M, Mustapha A. Antibacterial properties of selenium nanoparticles and their toxicity to Caco-2 cells. Food Control. 2017;77:17-24.
56. Tran PA, O'Brien-Simpson N, Reynolds EC, Pantarat N, Biswas DP, O'Connor AJ. Low cytotoxic trace element selenium nanoparticles and their differential antimicrobial properties against S.aureus and E. coli. Nanotechnology. 2015;27(4):045101.
57. Salem SS, Fouda MMG, Fouda A, Awad MA, Al-Olayan EM, Allam AA, et al. Antibacterial, Cytotoxicity and Larvicidal Activity of Green Synthesized Selenium Nanoparticles Using Penicillium corylophilum. J Cluster Sci. 2020;32(2):351-361.
58. Huang X, Chen X, Chen Q, Yu Q, Sun D, Liu J. Investigation of functional selenium nanoparticles as potent antimicrobial agents against superbugs. Acta Biomater. 2016;30:397-407.
59. Salah M, Elkabbany NAS, Partila AM. Evaluation of the cytotoxicity and antibacterial activity of nano-selenium prepared via gamma irradiation against cancer cell lines and bacterial species. Sci Rep. 2024;14(1).
60. Al Jahdaly BA, Al-Radadi NS, Eldin GMG, Almahri A, Ahmed MK, Shoueir K, et al. Selenium nanoparticles synthesized using an eco-friendly method: dye decolorization from aqueous solutions, cell viability, antioxidant, and antibacterial effectiveness. Journal of Materials Research and Technology. 2021;11:85-97.